G.U. Journal of Science
22(3): 183-196 (2009)

GUJS
www.gujs.org

EMP Fusion

Işık Kuntay♠

Wayne State University, Department of Chemical Engineering, USA

Received: 29.03.2009 Revised: 30.04.2009 Accepted: 25.05.2009

ABSTRACT

This paper introduces a novel fusion scheme, called EMP Fusion, which has the promise of achieving break-even and realizing commercial fusion power. The method is based on harnessing the power of an electromagnetic pulse generated by the now well-developed flux compression technology. The electromagnetic pulse acts as a means of both heating up the plasma and confining the plasma, eliminating intermediate steps. The EMP Fusion device is simpler compared to other fusion devices and this reduces capital and operating costs. Fuel used in the scheme is Lithium Deuteride, the fusion fuel with the least neutron production, and thus chances of radioactive pollution are significantly minimized as well. Numerical calculations have been performed to demonstrate the role of the Lorentz force in confining the superheated plasma, keeping plasma density at the levels needed for Lawson's criterion, and allowing ignition to be achieved.

Key Words: Fusion, Electromagnetic Pulse, Lithium Deuteride, Lawson's Criterion, Inertial Confinement Fusion, Clean Energy.

1. INTRODUCTION

The importance of utilizing alternative energy sources has been realized since many decades. Researchers have been looking for ways to generate energy from sources that are renewable and "clean". Since 1950s, fusion has been the ultimate goal of energy research as it is clean, its fuel is virtually unlimited, and it is the energy source of the stars.

Fusion is the process by which two light atomic nuclei combine to form a heavier nucleus. It is a better alternative to fission because it does not involve radioactive byproducts that are highly pollutant. However fusion does not naturally occur under earthly conditions. Atomic nuclei are positively charged and like charges repel each other. Each nucleus is surrounded by a Coulomb barrier that normally prevents the nuclei from coming too close to each other.

For nuclei to come together, they must exceed each others' Coulomb barriers. This requires very high energy nuclei that are found in the stars. However, if nuclei could be excited to the required energy levels, fusion could be accomplished on earth. A collision between intensely energetic nuclei will bring them so close that they will feel the strong attractive nuclear force. The two nuclei will come together, fuse, and form a heavier nucleus. In the process, some of the mass is converted into kinetic energy.

In Figure 1 the fusion process of Deuterium and Tritium nuclei, both isotopes of hydrogen, is depicted. When the two nuclei collide with sufficient energy, they fuse and form nucleus of Helium-5, an isotope of Helium. This nucleus promptly decays into a regular Helium-4 nucleus and a neutron. There is net energy release from this two-step reaction and the particles fly off with considerable amount of kinetic energy.

Since the net energy released from the fusion process is significant, scientists have focused on harnessing this energy for commercial use. However, doing this has proven to be a major challenge. Despite decades of research, no one has yet achieved a self-sustaining, thermonuclear fusion reaction.

In thermonuclear fusion, the "fuel" for the reaction is a plasma (a state of matter consisting almost entirely of ions and electrons) that is heated to millions of degrees. The energies of individual particles in the plasma are distributed with respect to the Maxwell-Boltzman distribution. According to this distribution, even at relatively low plasma temperatures, some particles will be at sufficient energy to overcome the Coulomb barrier and will fuse. Energy is released by these early fusion events in the form of fast moving particles.

♠Corresponding author, e-mail: xkuntay@yahoo.com

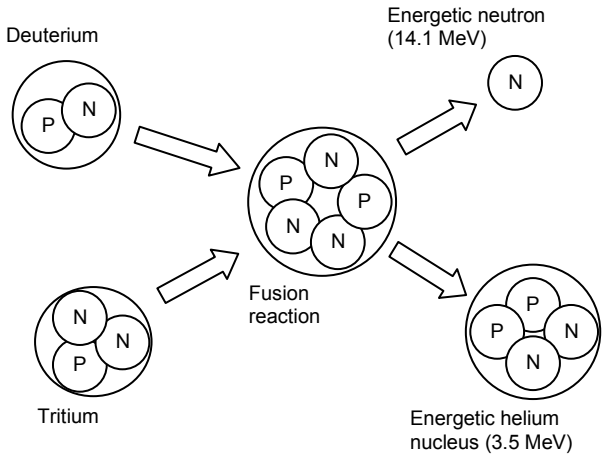

Figure 1. The reaction of D-T fusion with reactants and products.

If these particles are captured and become part of the plasma, the fusion process could become self-sustaining. The energetic particles would increase the average kinetic energy of the plasma and more fusion reactions would be triggered.

However, preserving the energy in the plasma turns out to be a major challenge. When an electron scatters and gets accelerated by an ion, energy is radiated away as continuum radiation, a process known as bremsstrahlung radiation. Such processes cool down the plasma and cease the fusion reactions. For the fusion to be self-sustaining, the rate of heat generation by fusion reactions must be larger than the cooling processes.

The energy gained by fusion and the energy lost through bremsstrahlung both have a temperature dependence. At a certain temperature these two will be equal and this is called the "ignition" temperature. Above the ignition temperature the plasma temperature is maintained and the fusion reaction becomes self-sustaining. For the DT reaction, the ignition temperature is about 4000 electron volts, or about 45 million degrees (one electron volt corresponds to about 11,600 kelvins).

Other loss mechanisms also cool down the plasma, but they are more amenable to experimental control. One is the loss of ions or electrons from the hot plasma. These carry energy away and the plasma cools. Another mechanism is also bremsstrahlung, but involves contaminants of "heavy" impurity ions, such as aluminum or iron. Since impurities are virtually always present due to the outgassing of walls and insulator materials that comprise the plasma chamber, minimizing impurities has been a major challenge for all fusion schemes up to date.

There are many other challenges in front of realizing a useful fusion process. However, even in the simplified picture of thermonuclear fusion depicted above, the level of difficulty is conspicuous. Any hindrance to the early fusion reactions in the plasma will prevent the ignition, and useful energy will not be generated. For any given temperature, the collision rate can be increased by increasing the plasma density. However, a high-temperature, high-density plasma exerts an outward pressure, and thus the higher the density, the more difficult it is to keep the plasma confined.

It is desirable to know whether or not a particular fusion scheme is feasible or not before any physical experiments are conducted. This evaluation can be done beforehand on paper by employing general assumptions and estimating the energies that would be generated by the plasma and lost by the plasma. The product of the density, n, and the plasma confinement time, t, that is, nt, is an important parameter in the evaluation, and the Lawson criterion states that a minimum value for nt be approximately 10^{14} sec-cm^{-3}.

2. BACKGROUND – THERMONUCLEAR FUSION AND EMP FUSION

The EMP Fusion method to be discussed in this paper is a type of thermonuclear fusion (as opposed to catalyzed fusion, or cold fusion). It is based on the facts discovered in earlier thermonuclear fusion studies.

2.1. Background of Thermonuclear Fusion

Thermonuclear fusion research in general can be grouped into two approaches. The first approach is to confine a low-density plasma. The plasma is then heated via methods such as direct currents, particle bombardment etc. and tried to be brought to the ignition temperature. The most eminent method with this approach is the tokamak, which is a toroidal reactor with magnetic fields that twist around its interior and keep the plasma confined in a donut shape. To date, billions of dollars have been spent on building, understanding, and developing tokamak reactors. Although tokamaks have occasionally met the Lawson criterion, they have failed to produce net energy.

The second approach to thermonuclear fusion is Inertial Confinement Fusion (ICF). In an ICF scheme, a sphere of solid deuterium and tritium is subjected on all sides to an imploding force that drives the DT fuel inward. The severe compression creates a hot, high-density plasma and results in fusion reactions. However, there is no way to confine the plasma once it is created, and the heat of the initial fusion events tend to expand the sphere and cool the plasma before ignition temperature is reached. It is only because the implosion occurs so quickly (in billionths of a second) that the inertia of the inwardly moving fuel is able to hold the sphere together and maintain the temperature. The confinement time, t, is on the order of only 10^{-11} seconds, which is balanced by the very high particle density (n ~ 10^{24} to 10^{25} cm^{-3}).

The most powerful implosions up to date have been performed at the Lawrence Livermore Laboratories with ultra-powerful laser machines. Ignition was achieved, but useful energy has still not yet been generated. There are also many issues with the production of the spherical targets, as any imperfection in the sphere causes the target to move and hit the wall of the "hohlraum", the metal cylinder in which it is

placed. This causes the plasma to be cooled or destroyed before ignition.

An alternative approach to thermonuclear fusion was proposed by Andrei Sakharov, involving elements of both ICF and tokamak. In this approach, a high temperature DT plasma is created under a strong magnetic field. The magnetic field confines the plasma similar to the tokamak. The confined plasma would then be imploded by an external force, similar to the process in ICF. The implosion would heat and compress the relatively dense plasma, and the strong field would help capture the energetic alpha particles produced during the fusion events.

This approach is called MAGO or Magnetized Target Fusion (MTF). The scheme was first tested in 1994 using a device involving a two-section chamber. A gas mixture of DT is introduced into both sections of the chamber. Two current pulses sent through the chamber cause a portion of the DT gas in one section to become ionized and then propelled through a nozzle so that it enters the second section at a very high velocity. The effect of the abrupt collision between this plasma, moving at hypersonic speeds, and the relatively static gas in front of it is to raise the temperature of the gas rapidly to several thousand electron volts. The created plasma was referred to as the target plasma.

In the second stage of the MAGO scheme, a very thin metal liner around the plasma chamber was shocked with an enormous current pulse. The liner then imploded because of the extreme magnetic field caused by the current, called the Lorentz force. This implosion increased both the temperature and the density of the target plasma. The plasma was indeed heated to close to ignition temperatures. However, the feasibility of the scheme is still under question.

The fusion scheme to be explained in this paper involves an approach similar to that of MAGO. However, the scheme is much simpler than any other fusion scheme thus mentioned. The fusion scheme is called EMP Fusion because it makes use of a high intensity Electromagnetic Pulse (EMP), which is explained below.

Since the work of Ampere and others in the late 18th century and early 19th century, people were aware that electrical currents always generated magnetic fields. The size of the current determined the field strength, and the field always pointed in a direction that was at right angles to the direction of current flow, which is known as the 'Right Hand Rule' (Figure 2).

However, it was not until 1831 that Michael Faraday showed the converse to be true; a changing magnetic field generates an electric field that causes a current to circulate in a conductor. Faraday summarized his observations by stating that a change in the "magnetic flux" that threaded a loop of wire would generate an electromotive force, that is, a voltage, which would induce current to flow. Figure 3 illustrates the concept of magnetic flux. While the flux can be defined and calculated for any arbitrary configuration of field and conductors, a simple case is shown in the figure. There, a uniform magnetic field passes straight through a circular loop of wire. The flux in this case is simply the field strength times the area of the loop. If the flux that threaded the loop changed, this would induce a current to flow in the wire. Since, as stated earlier, any current generates a magnetic field, a new magnetic field is also induced. Faraday demonstrated that the direction of that new field counteracts the change in the flux, a phenomenon that had been described, but not quantified, by Lenz's law. In other words, any attempt to change the flux through a conducting loop is counteracted by the induction of currents and fields that counter the flux change.

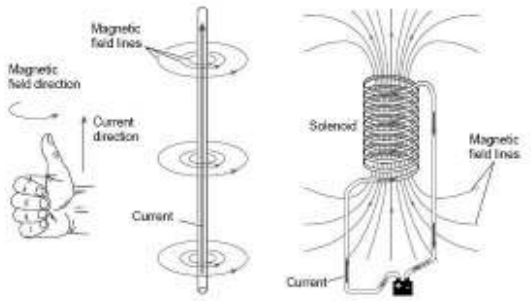

Figure 2. The explanation of the 'right-hand rule' for magnetic field generation.

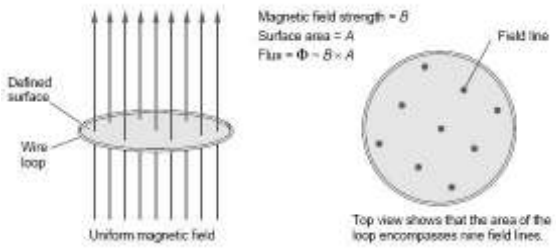

Figure 3. Explanation of magnetic flux.

If the loop were made from a perfectly conducting material, meaning that currents can circulate around that loop without losing energy, a change in the flux would induce a current that would be of sufficient strength to exactly counteract the change. As illustrated in Figure 4, the flux before and after will be the same, and the flux is said to be conserved. However, most materials are not perfect conductors but have some resistance. Current flowing through a copper or aluminum wire loses energy in the form of heat. An induced current continuously decays at some characteristic rate, which depends on both the resistivity of the material and the "inductance" of the loop, and therefore, the induced magnetic field also decays. It becomes unable to counteract the flux change to the full extent. On the time scale of an explosion, however, which may last only a few microseconds, a loop of a regular conductor maintains flux quite well. Thus, on minuscule time scales, shorter than the characteristic decay time, even normal materials approximate perfect conductors, and flux is approximately conserved.

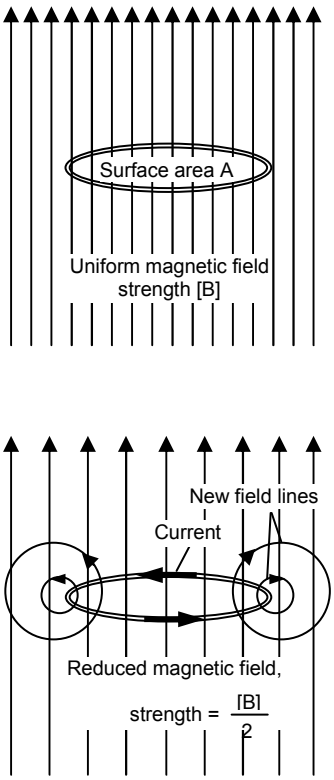

Figure 4. Faraday's Law and flux conservation.

Suppose that instead of the magnetic field through the loop being changed, the loop itself is changed and shrinks in size. The flux, which is proportional to both the field and the area, should decrease, but again, currents are generated in the conducting loop that create a new magnetic field that points in the same direction as the original field to counter the flux change. The total strength of the field threading the loop increases.

Flux compression generators use the principal of flux conservation and may use a hollow metal pipe instead of a wire loop and increase the field strength by modifying the shape of this conductor. The initial operation on the generator is to create an external field down the center of the pipe. Then, high explosives arranged symmetrically around the pipe will be detonated and the pipe will be rapidly compressed by the pressure of the explosion, causing the pipe wall to collapse towards the axis. On the short time scale of the explosion, the flux will be approximately conserved and remain relatively constant as the pipe cross section shrinks (Figure 5). The flux will be "compressed" because the same amount of flux will now occupy a significantly smaller area. To maintain the total flux, the magnetic field strength will increase to a great extent, and that increasing magnetic field, in turn, will generate a large current in the collapsing wall.

The high explosive plays a dual role in the scheme explained above. First, it collapses the conductor so quickly that flux conservation is approximated. Second, it is a source of energy. The energy of the explosive material comes from the chemical energy stored in the molecular bonds that make up the explosive which is converted to pressure when the explosive is detonated. Then that pressure does work on the conductor by compressing it. The conductor, in turn, does work on the field by compressing the flux magnetic field. Since the field magnitude increases, the energy content must also grow and that energy is stored in the magnetic field in proportion to the square of the field magnitude (B^2).

Today's flux compression generators are capable of 3000T magnetic field strength. The entire flux compression process powered by explosives lasts about 4 microseconds, but most of the compression takes place in the 1.5 microseconds before the explosive pressure subsides. Thus the magnetic field change rate could be approximated as 2000T/μs.

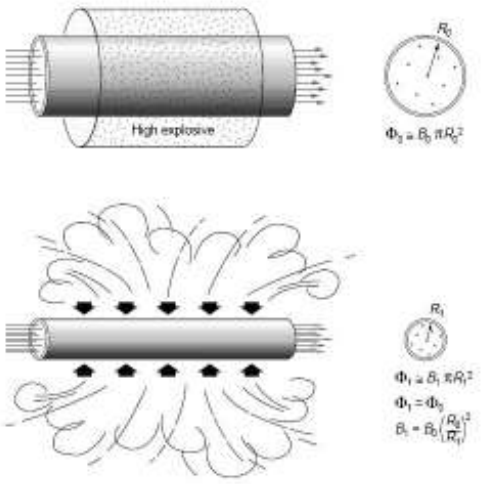

Figure 5. Explosive-Driven flux compression.

The EMP Fusion device is setup to harness this abrupt increase in the magnetic field. As Faraday's Law of Induction states, a changing magnetic field creates an electric current within the circuit through which it passes, such that the circuit tries to maintain the original magnetic field intensity. In EMP Fusion, the target is in a ring shape and placed at the end of an Explosively Pumped Flux Compression Generator (EPFCG). The ring depicted in Figure 6 is made entirely of Lithium Deuteride (LiD), the fuel of early hydrogen bombs. LiD has the highest deuterium (D) content for any material at normal conditions (i.e. room temperature and 1 atm).

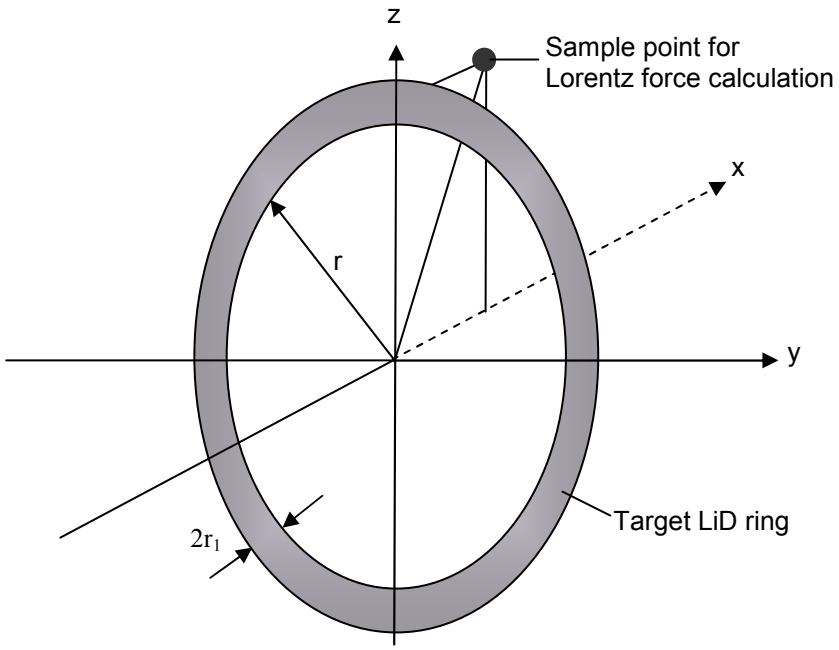

Figure 6. The structure of the target ring in EMP Fusion.

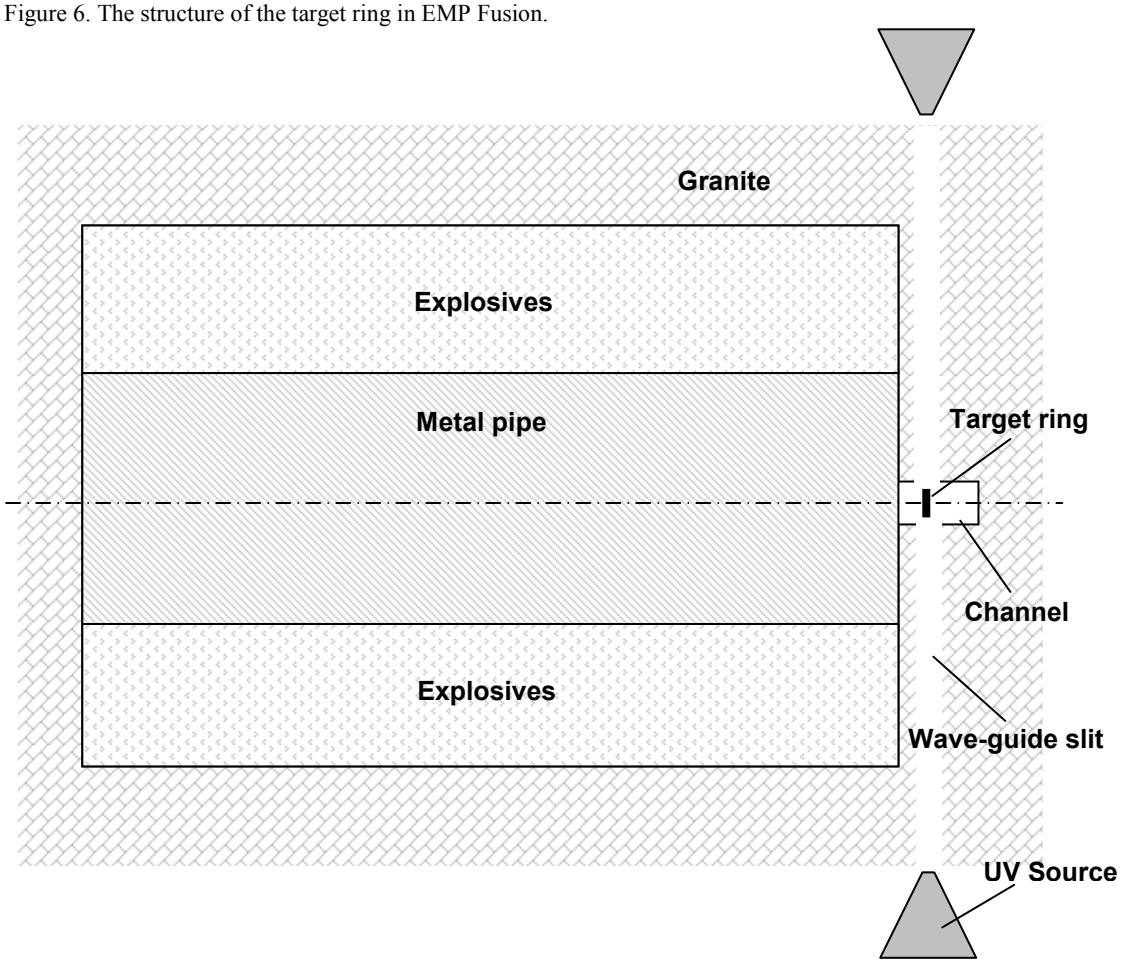

Figure 7. The EMP Fusion device setup.

2.2. EMP Fusion

Figure 7 depicts the EMP Fusion device studied in this paper. The device is made up of a large cylindrical chamber made from granite with a pipe at its center and explosives uniformly placed around the pipe, a small channel carved on the wall of the large chamber, and the target ring suspended without contacting the walls inside this channel. The granite block is sliced through the plane of the target ring and separated into two to form a 10 mm slit. Around the slit are UV lamps placed along the perimeter. The slit is vacuum sealed at the point of contact with the UV lamps. The interior of the pipe, the slit, and the channel are all vacuums prior to the operation. There are no conductive materials other than the EPFCG pipe and the ring within the device.

The EMP Fusion process is to be studied in two stages: Stage A) Before the lithium is fully ionized, and Stage B) After the lithium is fully ionized. The procedures and processes in these two stages are significantly different. Lithium deuteride melts at 964 K and boils at 1615 K. When it is liquid, it is a molten salt that has low electrical conductivity. Once it boils, it is a gas that no longer conducts electricity. For it to be influenced by an electric field, the gas has to be ionized. The ionization potential of lithium is 5.3 eV. Such an energy can easily be supplied through UV lamps of 230 nm wavelength that are commercially available. To fully ionize one mole of lithium gas to the primary ionization level, one needs to supply 520 kJ of energy. Each ionized lithium atom has a lifetime of about 103 ns. So, exposing 1 mole of lithium gas to 520 kJ of energy for 103 ns will fully ionized the gas. In the example in this paper, the amount of lithium is 0.096 moles, which means the energy needed to fully ionize the gas is 49.92 kJ. Dividing this by 103 ns, we get 484,660,194 kJ/s, or about 485 MW. This is gigantic power that would be expensive supply. However, instead a fully ionized gas, one can create partially ionized gas or "lionized" gas. If 485 MW fully ionize 0.096 moles of lithium, 0.5 MW should ionize about 0.1% of the gas. The next task is to estimate the conductivity of 0.1% ionized lithium gas. The electrical resistivity of fully ionized lithium gas is close to $5x10^{-6}$ ohm-m. The resistivity of 0.1% ionized lithium gas can then be approximated as $5x10^{-3}$ ohm-m. Since there are other factors that may increase the resistivity, such as the presence of deuterium, in this paper we will assume that the resistivity of 0.1% ionized lithium gas at 1615 K is 1 ohm-m and it gradually decreases to 0.0031 ohm-m at 55,000 K.

The EMP Fusion process is as follows, starting with Stage A:

1. An initial magnetic field of 200 Teslas is created inside the EPFCG device.
2. The target ring is slowly heated to 964 K by radiation.
3. The explosives surrounding the EPFCG pipe are detonated. At the same time, the radiation on the target ring is intensified.
4. Current is induced in the pipe, which compresses the magnetic field.
5. The target ring is initially in molten salt state and conducts weak currents. The changing magnetic field generates a current in the target ring.
6. Within 50 nanoseconds the target ring reaches 1615 K and becomes a gas.
7. The UV lamps are turned on and the target ring is radiated with UV rays. This ionizes the lithium gas in the target.
8. As the EPFCG device continues operation, the magnetic field intensifies.
9. The changing magnetic field induces currents in the ionized lithium, which generate heat. The strong magnetic field locks the ions and electrons and prevents them from spreading radially. This way the 'ring' shape of the target is preserved.
10. The power from the UV lamps together with the electric current heats up the gas.
11. As the temperature rises, pressure builds up in the gas and it expands. Since the surrounding is vacuum the expansion is very quick, but in the scale of nanoseconds, it is not enough to destroy the integrity of the gas. Again the strong magnetic fields restrict the expansion along the axis of the ring. The circuit is preserved and continues to conserve the magnetic field.
12. The UV lamps supply power until the gas has reached 55,000 K. Once this temperature is reached, lithium is fully ionized and becomes plasma. At this point the UV lamps are turned off. Stage B ensues.
13. The conductivity of the gas increases significantly with the transformation of lithium into plasma. However, the deuterium is still not ionized.
14. Strong currents flow in the plasma. The currents create Lorentz forces which keep the plasma together.
15. The increasing temperature also increases the conductivity of the plasma. The induced current rises and the Lorentz forces become stronger. As seen in the example, the Lorentz forces at some point exceed the expansion pressure.
16. At some point, the Lawson criterion is met and the plasma ignites. The ignition may create a massive heat wave that would destroy the plasma, but useful energy would already be generated. The heat can be collected as in standard nuclear reactors with heat exchangers and turned into electricity via steam turbines.

The main advantages of the EMP Fusion are:

a) The device is simple to operate and relatively inexpensive to construct.

b) The EMP has three roles:

-Heating the target

-Keeping the plasma together and confining the ions

-Compressing the plasma further

c) The heat losses are minimized by the absence of any convection or conduction around the target.

d) The walls of the channel in which the target resides act as a reflecting medium for the bremsstrahlung radiation.

e) There are no intermediate transmission lines for the transfer of energy from the EPFCG to the target ring. Energy is transferred directly and most efficiently.

f) The possibility of igniting more fuel with the heat from the ignition of the first target emerges. This might be accomplished by placing frozen deuterium at the back of the target channel.

g) The apparatus is tolerant to small imperfections in the target, chamber, or EPFCG.

h) The lithium in the target captures the hazardous neutrons and helps turn them into energy, thus preventing them from damaging surrounding equipment.

2.3. Process Model

The process of the operation of the EMP Fusion device has been modeled with some assumptions. The results show that Lorentz forces are more than sufficient to keep the plasma together and Lawson's criteria can easily be met at the end of the process. The following assumptions were made during the modeling of the process:

1. The expansion speed of the gas in stage A is constant and 34,000 m/s.
2. The EPFCG generates an EMP of 2000T/μs for 2 μs.
3. The magnetic flux change rate created by the EPFCG is constant.
4. Lithium becomes a fully ionized plasma at 55,000 K.
5. The plasma obeys the ideal gas law.
6. The resistivity of ionized lithium gas gradually drops from 1 ohm-m at 1615 K to 0.0031 ohm-m at 55,000 K as depicted in Figure 12.
7. The Lorentz force is calculated assuming the plasma can be separated into two rings with centers separated by a distance equal to the radius of the plasma.
8. The pressure exerted by the Lorentz force is the force divided by the vertical cross section of the main ring, or in terms of parameters, the perimeter of the ring multiplied by its thickness. This is reasonable following assumption 7.
9. The heat capacities of LiD and Li stay constant. This assumption leads to a deviation in temperature calculations. However, as the results will show, even a 500% deviation is affordable.
10. Expansion of the plasma is too slow to cause any cooling.
11. Lithium does not interfere with the fusion. Not only this assumption is likely but the contrary is also likely, that Lithium helps the fusion, as Lithium absorbs the neutrons and becomes tritium (T), another fusion reactant.
12. Time steps of 0.032 nanoseconds were taken for the calculation of the induced currents, heat generation, and Lorentz force. The current in one step was calculated based on the plasma surface radius from the previous step.
13. The net magnetic flux through the target ring is calculated by subtracting the magnetic field created by the currents in the ring from the magnetic field of the EPFCG. It is assumed that the increase in induced magnetic field cannot exceed one third of the increase in the EPFCG field. More explained in next assumption.
14. The current in the plasma cannot increase more than what would create a magnetic field change that is one third of the magnetic field change of the EPFCG. The explanation for this assumption will be given later.
15. The current in the plasma cannot decrease more than 5% at every time step. This is to prevent divergent oscillations from occurring during the simulation and does not affect the authenticity of the simulation.
16. The area and radius of the target ring stay constant. This assumption is reasonable since at a magnetic field of 200 T the radial Lorentz force, which is not to be confused with the Lorentz force arising from current, acting on an individual electron with 0.32 eV energy is 1.05×10^{-11} N, whereas the centrifugal force on an electron in an orbit of 0.00004 m and 1381 eV energy is 1.04×10^{-11} N. Clearly, with magnetic fields above 200 T no charged particle can escape its orbit even at 10 million K, assuming that each 11,604 K corresponds to 1 eV. Thus, the ring will be solidly locked in position until ignition. At 100 million K, if the magnetic field were in excess of 2000 T the ions would still be trapped in their orbits.

17. Target melts at 964 K and boils at 1615 K.

Table 1 lists the constants and initial parameters used in the calculations. Note that the calculations are only focusing on the target, as modeling the EPFCG requires additional data. However, EPFCG is a well understood device and obtaining the data is a matter of collaborating with the relevant institutions. The equations used in the calculations are as follows:

The current induced in the ring by the magnetic flux change is contingent upon the electromotive force (EMF) in Faraday's law of induction:

$$\varepsilon = - \frac{d\,\Phi_N}{d\,t} \tag{1}$$

where ε is the EMF in volts, Φ_N is the net magnetic flux through the circuit in webers, and t is time is seconds. The net magnetic flux is the area of the target ring times the net magnetic field:

$$\Phi_N = B_N A \tag{2}$$

where B_N is the net magnetic field strength in teslas, and A is the area of the ring, in meter squares. The net magnetic field is calculated as:

$$B_N = B_G - B_I \tag{3}$$

where B_G is the magnetic field created by the EPFCG and B_I is the opposing magnetic field generated by the induced currents in the target. The last term calculate from:

$$B_I = \frac{\mu_o I}{2\,r} \tag{4}$$

μo is the magnetic constant, I is the current in the target, and r is the radius of the target ring. The current is calculated from Ohm's law:

$$I = \frac{\varepsilon}{R} \tag{5}$$

where R is the resistance of the circuit measured in ohms.

Resistance in turn is computed as:

$$R = \frac{L\,\rho}{S} \tag{6}$$

where L is the length of the circuit in meters, ρ is the resistivity of the material in ohm-meter, and S is the cross-sectional area of the circuit in m^2.

The initial cross-sectional area is calculated from the initial parameters in Table 1. The Lorentz force is calculated from the formula:

$$F = I\mathbf{L}x\mathbf{B} \tag{7}$$

where I is the current in the circuit in amperes, from equation 5, **B** is the magnetic field vector in teslas, not to be confused with B_N, B_I or B_G, and **L** is the vector along the circuit with magnitude equal to the circuit's length in meters.

The Lorentz magnetic field per assumption 8 is generated on one half of the circuit by the other half. This magnetic field is calculated by the Biot-Savart law:

$$dB = \frac{\mu_o I}{4\pi} \frac{d\mathbf{S}x\mathbf{v}}{l^3} \tag{8}$$

where d**s** is a vector along the wire with differential length, **v** is the displacement unit vector in the direction pointing from the wire element towards the point at which the field is being computed, and l is the distance from the wire element to the point at which the field is being computed.

To calculate the magnetic field exerted on the second loop by the first loop, we can select a point on the second loop as shown in Figure 2. The magnetic field at each point on the conjugate ring is assumed equal. The infinitesimal wire element vector is given by the following formula:

$$d\mathbf{S} = 0\mathbf{i} + \sin\theta.r.d\theta\mathbf{j} - \cos\theta.r.d\theta\mathbf{k} \tag{9}$$

where θ is the angle in cylindrical coordinates of the point on the ring. The Cartesian coordinates of the point outside the ring is (Figure 2.) x = d, y = 0, z = r.

The displacement vector **v**, is given by:

$$\mathbf{v} = d\mathbf{i} - r\cos\theta\,\mathbf{j} + (r - r\sin\theta)\mathbf{k} \tag{10}$$

The cross product of the displacement is:

$$d\mathbf{S}x\mathbf{v} = (r^2\sin\theta d\theta - r^2 d\theta)\,\mathbf{i} - r\,d\cos\theta d\theta\,\mathbf{j} - r\,d\sin\theta d\theta\,\mathbf{k} \tag{11}$$

Our point of interest is the **k**-component of B, since the Lorentz force is perpendicular to this and the current vector. The **k**-component of B is given by:

$$B_k = \frac{\mu_o I}{4\pi} \int_0^{2\pi} \frac{r\,d\sin\theta d\theta}{(d^2 + r^2\cos^2\theta + (r - r\sin\theta)^2)^{3/2}} \tag{12}$$

Unfortunately there is no simple analytical solution to this equation. Thus, in the calculations, a numerical integration is utilized.

After Equation 12 is solved, Equation 7 can be utilized to find the Lorentz force. To find the pressure on the ring, the force is divided by the vertical cross-sectional area of the ring:

$$P = \frac{F}{L\, 2\, r_1} \tag{13}$$

where r_1 is the cross-sectional radius of the ring. The volume sustained by the plasma is calculated via the ideal gas law:

$$V = \frac{N\, R_I\, T}{P} \tag{14}$$

where N is the total number of moles in the gas taking into account the dissociation of LiD into its constituents ($N_1 + N_2$), and R_I is the ideal gas constant.

The temperature is calculated from the heat generation from ohmic heating and heat capacity of the plasma. The ohmic heating is given by:

$$Q = I^2 R \tag{15}$$

where R is given by Equation 6. The temperature rise then is:

$$\frac{dT}{dt} = \frac{Q}{(Cp_1N_1+Cp_2N_2)} \tag{16}$$

where Cp_1 and N_1 are the molar heat capacity and moles of component 1, and Cp_2 and N_2 are the molar heat capacity and moles of component 2. Since the calculations done were based on time steps, the variable is ΔT, the temperature rise in that time step:

$$\Delta T = \frac{Q}{(Cp_1N_1+Cp_2N_2)}\ \Delta t \tag{17}$$

Finally, the ion density is calculated so that Lawson's criterion can be checked. The ion density only applies to deuterium nuclei. The value is given by:

$$J = N_1 Av/V \tag{18}$$

where Av is the Avagadro's number, and V is the plasma volume in cm^3.

To prevent the current from rising too fast and creating a big reduction in or even a negative electromotive force in the next time step, the following inequality is used:

$$BI_{,j+1} \leq (BG_{,j+1} - BG_{,j})/\alpha f + BI_{,j} \tag{19}$$

where $B_{I,j+1}$ is the induced magnetic field from the time step j+1 and αf is the control factor to be determined during optimization.

To prove that the magnetic field is strong enough to confine the fast moving particles, the following equations are used:

$$\upsilon_p = \sqrt{\frac{2\, E_p}{m_p}} \tag{20}$$

$$F_c = \frac{2\, E_p}{r_o} \tag{21}$$

$$F_b = C_p\, \upsilon_p\, B\, N \tag{22}$$

where υ_p is the velocity of the particle in m/s, E_p is the energy of the particle in joules, mp is the mass of the particle in kg, F_c and F_b are respectively the centrifugal force and the Lorentz forces acting on the particle in N, r_o is the radius of the particle's orbit at equilibrium ($F_c = F_b$) in m, and Cp is the charge of the particle in C. Equations 20 – 22, however, were not used in the main simulation. This makes the simulation conservative.

3. NUMERICAL CALCULATIONS

To demonstrate the efficacy of the EMP Fusion scheme introduced in this paper, a case study was conducted based on certain target ring specifications. The calculations were performed based on the equations given in the previous section and by means of a Visual Basic program. The algorithm of the program is outlined in Figure 8.

The system parameters are given in Table 1. The ring is held in place by ultra thin strings of polymer hanging from the wall of the target channel. The EPFCG is a standard one, details of which are not given in this paper. The results of the simulation are displayed in Figures 9 – 12.

Figure 9 depicts the rise of plasma temperature with time. The time scale is given in nanosecond. The time it takes to reach 100 million K is 1476 nanoseconds. Stage B, or 55,000K is reached in 263 nanoseconds. The graph is almost flat during Stage A because the target is not yet a plasma and its resistivity is high. After the target has become a fully-ionized plasma the temperature rise is almost exponential in time.

Table 1. Constants and Starting Parameters in the Numerical Calculations.

Constant	Value	Units	Explanation
μo	0.00000126	T.m/A	Magnetic constant
R	8.3145	$m^3 \cdot Pa \cdot K^{-1} \cdot mol^{-1}$	Universal gas constant
ΔB/Δt	2 x 10^9	tesla/s	EPFCG flux change rate
r	0.04	m	Target ring radius
L	0.2512	m	Target ring perimeter
r_1	0.0008	m	Initial target thickness
ρ,i	1.0	ohm-m	Initial elec. resistivity
ρ_{120kK}	0.000001	ohm.m	Resistivity after 120000K
ND	0.039	moles	Moles of deuterium
NLi	0.061	moles	Moles of lithium
CpD	10.4	J/(mol K)	Heat capacity of D
CpLi	24.86	J/(mol K)	Heat capacity of Li
ExSpd	34000	m/s	Expansion speed in St. A
ECF	3.02		Current control factor
$T_{,i}$	1615	K	Initial temperature

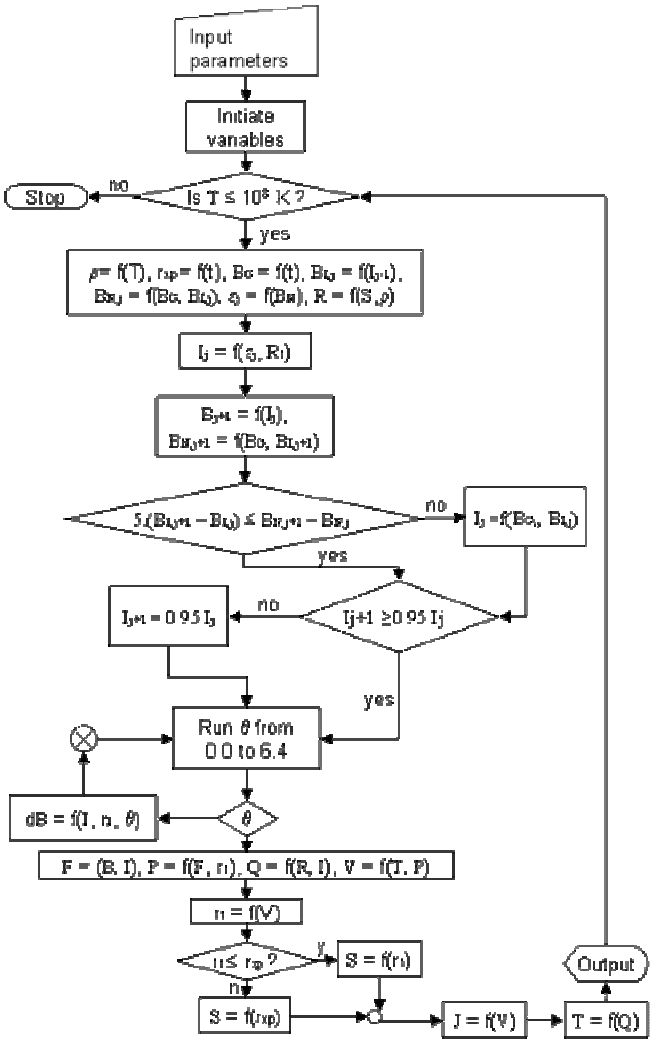

Figure 8. VB algorithm used for simulation of example case.

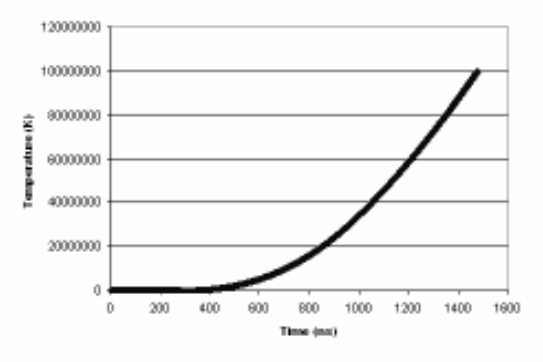

Figure 9. Temperature vs. time graph from the simulation.

Figure 10 depicts the total current induced in the target w.r.t. time. The current is small in Stage A, rises rapidly after the lithium fully ionizes, and then continues to rise with a slightly reducing slope. Although the graph in Figure 10 looks pretty smooth, when magnified, as in Figure 16, it could be seen that some parts of the curve are composed of two lines. These "forks" are not by mistake. If the graph is looked even closer, it could be seen that the current oscillates. This does not represent what would happen in reality. The oscillations are due to the nature of the numerical simulation.

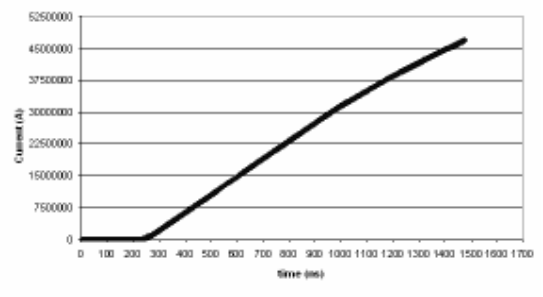

Figure 10. Current vs. time graph from the simulation.

There are two reasons for these oscillations. The first one is about plasma radius. In the calculations, the current in one time step is calculated based on the radius in the previous time step. If the plasma thickness in the previous time step were small, the current in the next time step would also be small, since resistance is inversely proportional to the thickness. In turn, a small current would result in smaller Lorentz force and that would cause the plasma to expand, increasing the thickness, and thus allowing higher current in the next time step.

The second reason is the net magnetic flux change in the target. If at one time step the current increases too rapidly, it will offset the EPFCG field by Equation 3. This means the EMF will be less in the next time step, and hence the current induced will be less. In reality the current would increase gradually and these kinds of oscillations would not occur. However, in the numerical calculations some oscillation is inevitable.

These oscillations in the simulation could in fact be reduced by smaller time steps, but that means more computation time. Another way to prevent oscillations is to limit the increase in current. This is a reasonable safety measure, since it is quite effective in restraining the oscillations, as seen from Figure 10, and it is in agreement with reality. The current is refrained from abrupt increases by means of Equation 19. Sudden decreases in current also lead to divergence, so no more than 5% decrease is permitted each time step as outlined in Figure 8. This is a realistic approximation.

In Figure 11 the change in the plasma radius could be seen. Again the two stages are conspicuously discernable. In Stage A, the plasma is assumed to expand at a constant rate. The assumed expansion rate, 34,000 m/s is quite reasonable as most blast waves travel with even smaller speeds. The aim of the target design is to have the target reach the plasma temperature before it is distorted. Distortion would occur if the crossectional radius, $r_{l,}$ was to exceed the ring radius, r. In Figure 11, it is seen that Stage B was reached before r_l even reached 0.018 m, quite smaller than r, which is 0.04 m. The factor of strong magnetic field in capturing the free ions and confining them in orbits with radii less than 0.00004 m was excluded from this simulation and could be added in future studies.

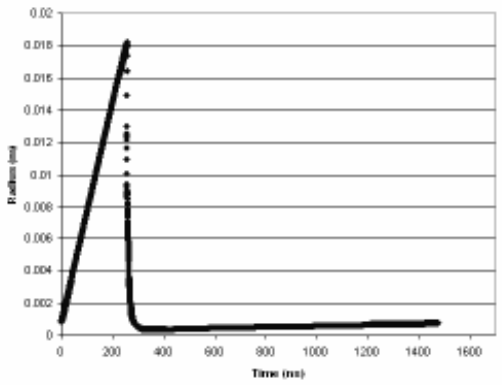

Figure 11. Plasma radius vs. time graph from the simulation.

At the point when lithium fully ionizes, electric currents quickly build up and the Lorentz force takes over the expansion pressure. Shortly after the 263th nanosecond, the plasma radius quickly drops below 0.001 m and stays in that vicinity for long time although temperature increases. The final plasma thickness at 100 million K is only about 0.0007 m, about the same as that of the original solid LiD ring.

Figure 12 shows the pressure exerted on the plasma by the Lorentz force. Again, pressure in Stage A is very small, close to zero. The shapes of pressure and current graphs are inherently very similar. The oscillations in current also create the oscillations in Lorentz pressure. The final pressure in the order of 10^9 atm is significant.

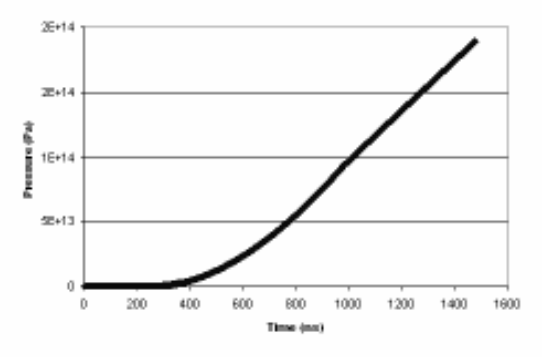

Figure 12. Pressure vs. time graph from the simulation.

The data for the conductivity of the deuterium-lithium gas and plasma were not available since these types of studies were not published. However, after reviewing information from other studies on resistivities of hot plasmas and ionized gases, some general assumptions were made. Figure 13 shows the resistivities used at different temperatures. The starting temperature is 1615 K degrees at which temperature the resistivity is 1 ohm-m. The resistivity gradually drops to 0.003 ohm-m at 55,000 K, 0.00001 ohm-m at 100,000K, and $1x10^{-6}$ ohm-m at 120,000K, the plasma temperature of deuterium. It is then assumed to be constant at $1x10^{-6}$ ohm-m for the rest of the time. This assumption is conservative since it is possible for the resistivity to drop further.

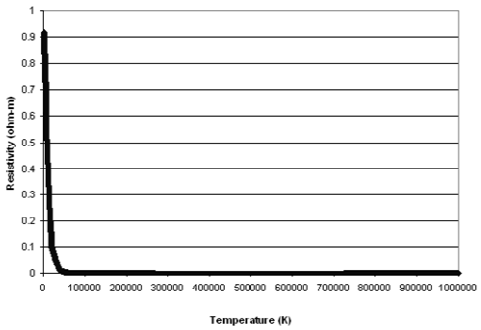

Figure 13. Resistivity vs. temperature correlation used in the example.

The final calculation is the Lawson's criterion, which is the product of the plasma density and the confinement time. The plasma density is given in Figure 14. As explained in Equation 18, the plasma density is based on deuterium and excludes lithium. It is worthwhile to mention the spike in plasma density around 260 nanoseconds. This spike is caused by the abrupt implosion of the gas right after the full ionization of lithium. The final 200 nanosecond will be chosen for Lawson's criterion because the ignition is likely to take place at 80,000,000 K. The lowest plasma density in the last 200 nanoseconds is $5.3x10^{22}/cm^3$. The product of the plasma density and confinement time yields 1.06 x 10^{16} sec-cm^{-3}. This proves that EMP Fusion may meet Lawson's criterion.

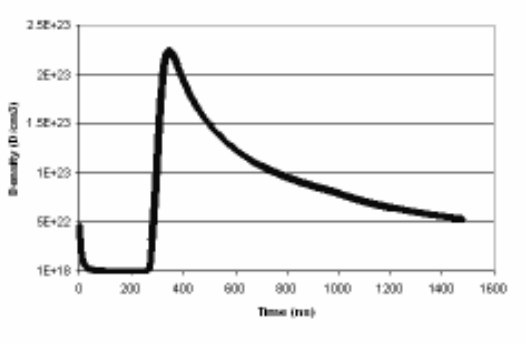

Figure 14. Plasma density vs. time from the simulation.

The oddest looking graph is Figure 15, which shows the induced electromotive force versus time. This graph is characterized by extensive oscillations. These oscillations are caused by small fluctuations in current. A restrained increase in current can cause the induced EMF in next time step to be very large. However, it is not realistic to expect the current to respond to such abrupt changes instantly, so these oscillations are filtered by Equation 19 and only shown in Figure 15.

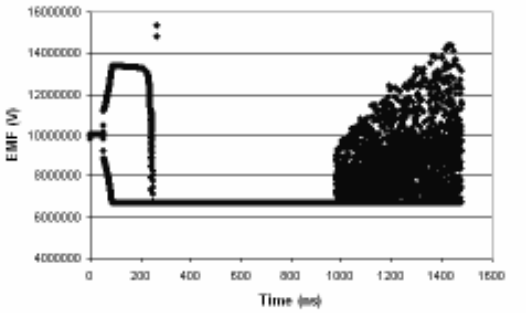

Figure 15. Electromotive force generated vs. time from the simulation.

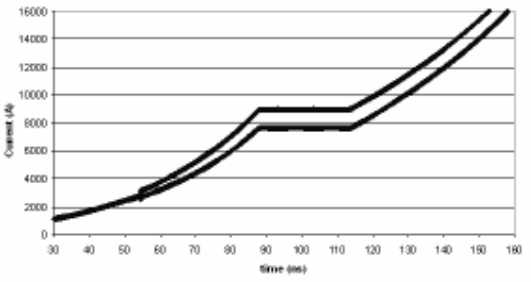

Figure 16. Close-up of current-time graph and oscillations.

4. DISCUSSIONS AND CONCLUSIONS

EMP Fusion has undeniable resemblance with early Z-pinch fusion experiments in the 1960s, which involved passing a strong current through a metal pipe that accommodated the deuterium-tritium plasma. Those experiments had failed because the plasma broke into blobs and restricted the flow of current shortly after the initial current was imposed. This led the scientists to improve the early design to the current Z-pinch method involving an external plasma that compresses the fusion fuel at its center in a process similar to that in ICF. It is true that both in EMP Fusion and early Z-pinch the means of plasma confinement is the Lorentz force. However, in EMP fusion the current flows in circles as opposed to on a single axis. In addition, in EMP Fusion the current is created with a changing magnetic field. Even if the plasma were broken into blobs, this would not stop the current, since plasma is made up of nuclei and electrons which respond to magnetic field. Instead, the blobs would fuse back together with the effect of the Lorentz force, thus maintaining the unity of the plasma. Also, electrons and nuclei move in opposite directions and the particles accelerate faster in unoccupied space. These are advantages of EMP Fusion over early Z-pinch. The most notable difference may be the presence of a strong perpendicular magnetic field. This field confines individual particles into orbits that are within the spatial vicinity of the original target ring. These are all factors that prevent the plasma from breaking up and permit stable plasma to be formed.

The results of the simulation show that EMP Fusion is a promising scheme. EMP is able to produce the temperature and pressure required for self-sustaining fusion in the target. The simplicity of the device and the efficiency of the energy transfer supports EMP Fusion's candidacy for a commercially feasible fusion energy technology.

As a future research, smaller time steps or smaller angular steps for the integration could be used to improve simulation resolution, improved models for EPFCG and heat capacities could be utilized, and the simulations could be performed with different fuel geometries, the results compared and and the one with the maximum energy yield studied further. Ways to model the resistivity of plasma at high temperatures could also be investigated.

Studies to be conducted on the EMP Fusion scheme include cases with different fuel compositions. These could be targets with frozen D-T cores and lithium shells, or pure D-T targets with more powerful UV lamps. Another possibility is employing two EPFCGs, one on each side of the target ring and both with magnetic fields in same direction. The shock from the first EPFCG can create a pressure in excess of 4 million atm, the metallization pressure of deuterium, on the shell. Right at metallization the second EPFCG could be operated, directly heating up the D-T mixture up to the ignition temperature. Overall, there are many optimization studies to be performed on this novel thermonuclear fusion scheme.

REFERENCES

[1] Younger, S., Lindemuth, I., Reinovsky, R., Fowler, C.M., Goforth, J., Ekdahl, C., "Scientific collaborations between Los Alamos and Arzamas-16 using explosive-driven flux compression generators", ***Los Alamos Science***, 24 (1996).

[2] Lindemuth, I.R., (Eds.) "Proceedings from the 1st International Symposium for Evaluation of Current Trends in Fusion Research: *Magnetized Target Fusion – An Ultra High Energy Approach in an Unexplored Parameter Space",* Washington, DC. (1994).

[3] Wessling, F.C., Moser, M.D., Blackwood, J.M., "Subtle issues in the measurement of the thermal conductivity of vacuum insulation panels", ***Journal of Heat Transfer,*** 126: 155-160 (2004).

[4] Shilkin, N., Dudin, S., Gryaznov, V., Mintsev, V., Fortov, V., "Measurements of the electron concentration and conductivity of a partially ionized inert gas plasma", ***Journal of Experimental and Theoretical Physics,*** 97(5): 922-931 (10) (2003).

[5] Mitchner, M., Kruger, C.H., "Partially Ionized Gases", ***John Wiley & Sons Inc.***, San Francisco (1973).

[6] Boyd, R.W., Dodd, J.G., Krasinskit, J., Stroud, C.R., "Disk-shaped heat-pipe oven used for lithium excited-state lifetime measurements", ***Optics Letters***, 5(3): 117-119 (1980).

[7] Muggli, P., Hoffman, J.R., Marsh, K.A., Wang, S., Clayton, C.E., Katsouleas, T.C., Joshi, C., "Lithium Plasma Sources for Acceleration and Focusing of Ultra-relativistic Electron Beam", ***Proceedings from the '99 Particle Accelerator Conference: New York***, NY (1999).

[8] Gatilov, L.A., Ibragimov, R.A., Kudashov, A.V., "Structure of a detonation wave in cast TNT", ***Combustion, Explosion and Shock Waves,*** 25 (2): 206-208 (1989).

[9] Albares, F.J., Krall, N.A., Oxley, C.L., "Rayleigh Taylor instability in a stabilized linear pinch tube", ***Physics of Fluids***, 4: 1031-1036 (1961).

[10] Ney, P., Rahman, H.U., Wessel, F.J., Rostoker, N., "Staged Z Pinch", ***Physical Review Letters***, 74: 714-717 (1997).

[11] Bott, S.C., Haas, D.M., Eshaq, Y., Ueda, U., Lebedev, S.V., Chittenden, J.P., Palmer, J.B.A., Bland, S.N., Hall, G.N., Ampleford, D.J., Beg, F.N., "Quantitative measurements of wire ablation in tungsten X-pinches at 80 kA", ***IEEE Transactions on Plasma Science***, 36 (3): 2759-2764 (2008).

[12] Yamanaka, C., "Inertial confinement fusion: The quest for ignition and energy gain using indirect drive", ***Nuclear Fusion***, 39: 825-827 (1999).

[13] Ahlborn, B., Key, M.H., Bell, A.R., "An analytic model for laser-driven ablative implosion of spherical shell targets", ***Physics of Fluids***, 25: 541 (1982).

[14] Pfalzner, S., Cowley, S., "An Introduction to Inertial Confinement Fusion", ***Oxfordshire: Taylor and Francis*** (2006).

[15] Niederhaus, J., Ranjan, D., Oakley, J., Anderson, M., Bonazza, R., "Inertial-fusion-related hydrodynamic instabilities in a spherical gas bubble accelerated by a planar shock wave", ***Fusion Science and Technology***, 47(4): 1160 (2005).

[16] Bültmann, S., Crabb, D.G., Day, D.B., Fatemi, R.D., Gardner, B., Harris, C.M., Johnson, J.R., McCarthy, J.S., McKee, P.M., Meyer, W., Penttilä, S.I., Ponikvar, E., Rijllart, A., Rondon, O.A., Lorant, S.S., Tobias, W.A., Trentalange, S., Zhu, H., Zihlmann, B., Zimmermann, D., "A study of lithium deuteride as a material for a polarized target", ***Nuclear Instruments and Methods in Physics Research Section A***, 425: 1-2, 23-36 (1999).

[17] Borisov, N.S., Fedorov, A.N., Lazarev, A.B., Matafonov, V.N., Neganov, A.B., Plis, Y.A., Shilov, S.N., Usov, Y.A., Bazhanov, N.A., Kovalev, A.I., Gurevich, G.M., Dzyubak, A.P., Karnaukhov, I.M., Lukhanin, A.A., Černy, J., Wilhelm, I., Janout, Z., Šimane, C., Vognar, M., Ball, J., Durand, G., Lehar, F., Sans, J.L., "Frozen spin solid targets developed at the Laboratory of Nuclear Problems", ***Czechoslovak Journal of Physics Supplement***, 50(1): 401-408 (1999).

[18] Veleckis, E., "Thermodynamics of the lithium-lithium deuteride system", ***Journal of Physical Chemistry***, 81(6): 526-531 (1977).

[19] Rosenbluth, M.N., "New ideas in Tokamak confinement", ***Maryland: AIP Press*** (1994).

[20] Sarkar, P., Braidwood, S.W., Smith, I.R., Novac, B.M., Miller, R.A., Craven, R.M., "A Compact Battery-Powered Half-Megavolt Transformer System for EMP Generation", ***Plasma Science***, 34 (5): 1832-1837(2006).